Spin qubit relaxation in a moving quantum dot

Peihao Huang* and Xuedong Hu
Department of Physics, University at Buffalo, SUNY, Buffalo, New York 14260, USA
(Received 30 September 2012; revised manuscript received 20 June 2013; published 1 August 2013)

Long-range quantum communication for spin qubits is an important open problem. Here we study decoherence of an electron spin qubit that is being transported in a moving quantum dot. We focus on spin decoherence due to spin-orbit interaction and a random electric potential. We find that at the lowest order, the motion induces longitudinal spin relaxation, with a rate linear in the dot velocity. Our calculated spin relaxation time ranges from sub μs in GaAs to above ms in Si, making this relaxation a significant decoherence channel. Our results also give clear indications on how to reduce the decoherence effect of electron motion.

DOI: 10.1103/PhysRevB.88.075301 PACS number(s): 72.25.Rb, 03.67.Hk, 03.67.Lx, 72.25.Dc

I. INTRODUCTION

Over the past decade, there has been tremendous progress in the experimental study and theoretical investigation of spin qubit manipulation and decoherence.[1,2] An important advantage of electron spin qubits is that they can be coupled strongly via the exchange interaction,[3] which allows fast two-spin gates. However, exchange interaction is short-ranged, and long-range quantum communication remains a significant open problem in the scale-up of spin qubit architectures.

Various ideas have been proposed to move spin information on chip, such as via spin-photon coupling,[4,5] spin bus,[6] and directly moving the electrons themselves.[7–10] Spin-photon conversion is difficult because the strongest estimated coupling strength is still only in the order of MHz,[5,11] which is slower than or comparable to the spin dephasing rate in most materials. Spin buses, on the other hand, are limited by the energy gap between the bus ground state(s) and the excited states,[6,12] and are most useful for short-distance (up to a few microns) quantum information transfer. Comparatively, direct spin transport is attractive because of its conceptual simplicity and its similarity to the conventional charge-coupled devices. Indeed, several experimental groups have recently shown how a surface acoustic wave (SAW) can controllably transport an electron over several microns.[13–17] Clearly, transferring spin information by directly moving its carrier is an intriguing and promising approach, and deserves further in-depth analysis. Here we focus on the aspect of spin decoherence due to electron motion.

The main decoherence channel for a confined electron spin in a finite field is the hyperfine (HF) interaction induced pure dephasing.[18,19] Spin relaxation due to spin-orbit (SO) interaction is much slower.[20] On the other hand, spin relaxation of free electrons and holes in semiconductors is dominated by SO interaction,[21,22] while the effect of hyperfine interaction is strongly suppressed by motional narrowing.[22] For a moving electron spin qubit with controlled motion, an intriguing question is thus when decoherence due to SO interaction becomes dominant.

In this paper we study spin decoherence of a moving but confined electron due to static disorders in a semiconductor heterostructure. For example, in a modulation-doped GaAs/$Al_xGa_{1-x}As$ structure, the ionized dopants produce a random electric potential at the GaAs interface where the quantum dot (QD) is located. If the QD is moved along the interface, the electron spin can sense this random potential through the SO interaction, and undergo decoherence. The static disorder has been considered in the problem of spin relaxation of 2D electrons,[23,24] while we focus on its effect on confined (albeit moving) electrons. Here we construct a theoretical description of this decoherence mechanism. We find that this is a longitudinal relaxation channel at the lowest order. Its rate can be as fast as sub-μs in GaAs or above ms in Si, making it a significant decoherence channel.

II. ELECTRON HAMILTONIAN

The model system we consider is a single electron in a gate-defined QD from a two-dimensional electron gas (2DEG). In general the growth-direction confinement is much stronger, so that the QD can only be moved in the in-plane direction by programming the top gate potentials. The electron remains confined while the QD is moved. Indeed, we assume the QD motion is adiabatic so that the electron remains in the ground orbital state.

As shown in Fig. 1, we consider a uniform linear motion of the QD with a constant velocity $\boldsymbol{v}_0$ (the QD potential minimum is at $\boldsymbol{r}_0(t) = \boldsymbol{v}_0 t = [x_0(t), y_0(t)]$). Such a linear motion is possible in principle by programming the surface gate potential along the path of QD motion.[8,10] Alternatively, SAW has been shown to be effective in moving a single electron from one QD to another at the speed of sound.[7,13–17] In both these cases, the QD motion is facilitated by an external agent (external electrical control in the former, and the piezoelectric generator of the SAW in the latter). As such, the complete problem of the electron dynamics in a moving quantum dot is that for an open system, where the reservoir (or the external driving agent) is complex and difficult to define completely and quantum mechanically. In the present study, in order to simplify the problem, we assume that the reservoir, or the external driving agent, is classical and Markovian. In other words, the driving agent is so large that it does not remember any energy exchange with the electron. The consequences of this assumption will be discussed later in the manuscript. The Hamiltonian for the QD-confined electron is

$$H = H_d + H_Z + H_{SO} + \delta V(\boldsymbol{r}), \tag{1}$$

$$H_d = \frac{\boldsymbol{\pi}^2}{2m^*} + U(\boldsymbol{r} - \boldsymbol{r}_0(t)), \tag{2}$$

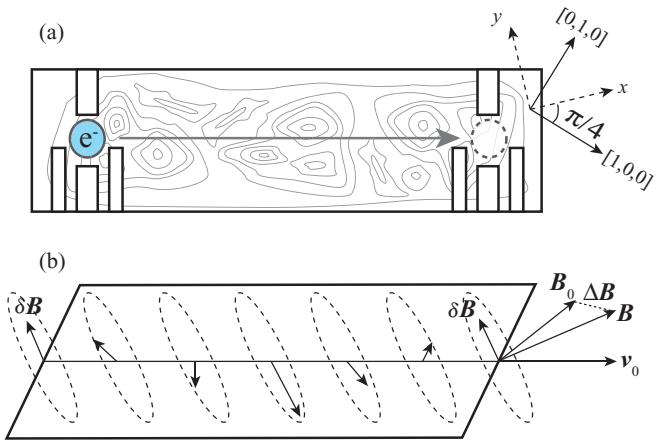

FIG. 1. (Color online) A schematic of a spin qubit in a moving QD. Panel (a) gives the top view of the structure and the coordinate system (xyz) defined in the laboratory frame, with x and y along the [110] and [$\bar{1}$10] directions. Panel (b) gives the side view and the total effective magnetic field.

$$H_Z = \frac{1}{2} g\mu_B \boldsymbol{B}_0 \cdot \boldsymbol{\sigma}, \tag{3}$$

$$H_{SO} = \beta_- \pi_y \sigma_x + \beta_+ \pi_x \sigma_y, \tag{4}$$

where $\delta V(\boldsymbol{r})$ represents a random electric potential, which is always present, whether due to modulation doping or barrier disorder. The subscripts d, Z, and SO refer to "dot," "Zeeman," and "spin-orbit." In H_d, $\boldsymbol{\pi}$ is the electron 2D momentum ($e > 0$) given by $\boldsymbol{\pi} = -i\hbar\nabla + (e/c)\boldsymbol{A}(\boldsymbol{r})$, and $U(\boldsymbol{r} - \boldsymbol{r}_0(t))$ is the dot confinement potential with a moving minimum $\boldsymbol{r}_0(t) = [x_0(t), y_0(t)]$. In this study, we consider a uniform linear motion of the QD, where $\boldsymbol{v}_0 = \boldsymbol{p}_0/m^* = d\boldsymbol{r}_0(t)/dt$ is a constant vector. In H_Z, $\boldsymbol{B}_0$ is the applied magnetic field (with $\hat{\boldsymbol{n}}_0$ its unit vector). In H_{SO}, $\beta_\pm \equiv (\beta \pm \alpha)$, where α and β are the Rashba and Dresselhaus SO coupling constants. The x and y axes are along the [110] and [$\bar{1}$10] directions. If x and y had been defined along the [100] and [010] directions, the SO term would have taken the usual form $H_{SO} = \beta(-\pi_x\sigma_x + \pi_y\sigma_y) + \alpha(\pi_x\sigma_y - \pi_y\sigma_x)$. The current choice of x and y helps simplify the presentation below.

To simplify the following treatment, we transform into the moving reference frame, so that the QD confinement potential becomes time independent. It is done by a translational transformation $|\psi'(t)\rangle = \exp[S_T(t)]|\psi(t)\rangle$, where the generator is $S_T(t) \equiv i\boldsymbol{\pi} \cdot \boldsymbol{r}_0(t)/\hbar$. The Schrödinger equation after the transformation is

$$i\hbar \frac{\partial}{\partial t}|\psi'(t)\rangle = H'|\psi'(t)\rangle, \tag{5}$$

in which the new Hamiltonian is $H' = e^{S_T} H e^{-S_T} + i\hbar\partial_t S_T$. After the transformation, the total Hamiltonian in the moving frame is

$$H' = H'_d + H'_Z + H'_{SO} + \delta V(\boldsymbol{r}_0(t) + \boldsymbol{r}'), \tag{6}$$

$$H'_d = \frac{\boldsymbol{\pi}'^2}{2m^*} + U(\boldsymbol{r}'), \tag{7}$$

$$H'_Z = \frac{1}{2} g\mu_B \boldsymbol{B} \cdot \boldsymbol{\sigma}, \tag{8}$$

$$H'_{SO} = \beta_- \pi'_{y'} \sigma_{x'} + \beta_+ \pi'_{x'} \sigma_{y'}. \tag{9}$$

Here $\boldsymbol{r}' = [x', y']$ and $\boldsymbol{\pi}'$ are the electron two-dimensional position and momentum operators in the moving reference frame. Operators in different frames are related: $\boldsymbol{r} = \boldsymbol{r}' + \boldsymbol{r}_0(t)$ with $\boldsymbol{r}_0(t) = \boldsymbol{v}_0 t$ and $\boldsymbol{\pi}' \equiv -i\hbar\nabla' + (e/c)\boldsymbol{A}(\boldsymbol{r}') - \boldsymbol{p}_L - \boldsymbol{p}_0$, in which $\boldsymbol{p}_L(t) \equiv -eB_{0z}/c[-y_0(t), x_0(t), 0]$ captures the effect of the Lorentz force (note that the classical motion of electron satisfies $\frac{d\boldsymbol{p}}{dt} = -e/c\boldsymbol{v}_0 \times \boldsymbol{B}_0 = \frac{d\boldsymbol{p}_L}{dt}$). In the moving frame, the random potential is time dependent due to the QD motion, $\delta V = \delta V(\boldsymbol{r}_0(t) + \boldsymbol{r}')$, so that the static disorder is now a charge noise. In H_d, $U(\boldsymbol{r}')$ is the time-independent confinement potential in the moving frame. In H_Z, $\boldsymbol{B} = \boldsymbol{B}_0 + \Delta\boldsymbol{B}$ is the total magnetic field, in which $\Delta\boldsymbol{B}$ is an effective magnetic field due to SO interaction in the moving reference frame

$$\Delta\boldsymbol{B} = \frac{2m^* v_0}{g\mu_B}(\beta_- \sin\phi_v, \beta_+ \cos\phi_v, 0), \tag{10}$$

where ϕ_v is the angle between the dot velocity and the [110] crystal axis. The Zeeman frequency is $\omega_Z = g\mu_B B/\hbar$ and the spin quantization direction is $\hat{\boldsymbol{n}} = \boldsymbol{B}/B$, which is generally different from the direction of the applied magnetic field $\boldsymbol{B}_0$.

III. CONSTRUCTING THE EFFECTIVE SPIN HAMILTONIAN FOR A MOVING ELECTRON

As the quantum dot is moved in a semiconductor heterostructure, the spatially random electrical potential $\delta V(\boldsymbol{r}_0 + \boldsymbol{r}')$ causes the momentum of the QD-confined electron to fluctuate. The electron spin can sense these momentum fluctuations via the spin-orbit Hamiltonian (9), and spin decoherence ensues. The QD motion we consider here is sufficiently slow so that it does not lead to any orbital excitation. We can focus on the electron spin dynamics by decoupling the spin space (with the ground orbital state) from the rest of the Hilbert space.[20,25–28] Specifically, we perform a Schrieffer-Wolff transformation $\tilde{H} = e^S H e^{-S}$ to remove the SO coupling in the leading order by requiring that $[H'_d + H'_Z, S] = H'_{SO}$.[20,25,26] For the harmonic confinement $U(r') = \frac{1}{2}m^*\omega_d^2 r'^2$, the SO term can be expressed as $H'_{SO} = i\mathbb{L}_d(\boldsymbol{\sigma} \cdot \boldsymbol{\xi})$, where $\mathbb{L}_d A \equiv [H'_d, A]$, $\forall A$ and $\boldsymbol{\xi} \equiv (y'/\lambda_-, x'/\lambda_+, 0)$ is a vector in the 2DEG plane; $\lambda_\pm \equiv \hbar/(m^*\beta_\pm)$ are the spin-orbit lengths. The superoperator $\mathbb{L}_d$ satisfies $\mathbb{L}_d^{-1}\boldsymbol{\pi}' = im^*\boldsymbol{r}'/\hbar$, and $\mathbb{L}_d^{-1}[x', y'] = -i(\hbar m^*\omega_d^2)^{-1}[(\pi'_{x'} + m^*\omega_c y'), (\pi'_{y'} - m^*\omega_c x')]$, where $E_Z = g\mu_B B$ is the electron Zeeman splitting (with $\omega_Z \equiv E_Z/\hbar$ being the Zeeman frequency) and $\omega_c \equiv eB_{0z}/(m^*c)$ is the cyclotron frequency. Assuming that the Zeeman energy is much larger than the SO energy, but much smaller than the orbital excitation energy ($m^*(\beta^2 + \alpha^2) \ll \hbar\omega_Z \ll \hbar\omega_d$), we get[20,25,26]

$$S = i\boldsymbol{\sigma} \cdot \boldsymbol{\xi} + E_Z(\hat{\boldsymbol{n}} \times \mathbb{L}_d^{-1}\boldsymbol{\xi}) \cdot \boldsymbol{\sigma}. \tag{11}$$

The transformed Hamiltonian is thus

$$H'' = i\hbar\partial_t S + H'_d + H'_Z + [S, \delta V(\boldsymbol{r})] + \ldots, \tag{12}$$

in which $i\hbar\partial_t S = \frac{1}{2}g\mu_B \Delta\boldsymbol{B}_L \cdot \boldsymbol{\sigma}$ with $\Delta\boldsymbol{B}_L = \frac{\omega_Z\omega_c}{\omega_d^2}\hat{\boldsymbol{n}} \times \frac{2\hbar}{g\mu_B}[v_{0x}/\lambda_-, -v_{0y}/\lambda_+, 0]$ being the high order correction of $\Delta\boldsymbol{B}$ which will be dropped in the following discussion.

The first order term due to the random electric potential is $[S, \delta V(\boldsymbol{r})] = \frac{1}{2}g\mu_B 2\boldsymbol{B} \times \boldsymbol{\Omega}(\boldsymbol{r}) \cdot \boldsymbol{\sigma}$, in which

$$\boldsymbol{\Omega}(\boldsymbol{r}) = \frac{-e}{m^*\omega_d^2}[\varepsilon_{y'}(\boldsymbol{r})/\lambda_-, \varepsilon_{x'}(\boldsymbol{r})/\lambda_+, 0], \tag{13}$$

where the electric field corresponding to the random potential is $\boldsymbol{\varepsilon}(\boldsymbol{r}) = \frac{1}{e}\nabla\delta V(\boldsymbol{r})$ $(e > 0)$. Therefore, the effective spin Hamiltonian takes the form

$$H_{\text{eff}} = \tfrac{1}{2} g\mu_B(\boldsymbol{B} + \delta\boldsymbol{B}(t))\cdot\boldsymbol{\sigma}, \tag{14}$$

$$\delta\boldsymbol{B}(t) = 2\boldsymbol{B}\times\boldsymbol{\Omega}(t), \tag{15}$$

$$\boldsymbol{\Omega}(t) = \langle\psi|\boldsymbol{\Omega}(\boldsymbol{r}_0(t) + \boldsymbol{r}')|\psi\rangle, \tag{16}$$

where $|\psi\rangle$ is the orbital wave function. To further simplify Eq. (16), we expand the random electric field $\varepsilon_i(\boldsymbol{r})$ $(i = x', y')$ around the average QD position $\boldsymbol{r}_0$,

$$\varepsilon_i(\boldsymbol{r}) \approx \varepsilon_i(\boldsymbol{r}_0) + \nabla\varepsilon_i(\boldsymbol{r}_0)\cdot\boldsymbol{r}' + \frac{1}{2!}\nabla\nabla\varepsilon_i(\boldsymbol{r}_0)\cdot\boldsymbol{r}'\cdot\boldsymbol{r}' + \ldots.$$

Due to the adiabatic condition, the electron always remains in the instantaneous ground orbital state $\psi(\boldsymbol{r}') = \exp(-r'^2/2\lambda^2)/\lambda\sqrt{\pi}$, up to a magnetic phase that does not affect the calculation of Ω. Here $\lambda^{-2} = \hbar^{-1}\sqrt{(m^*\omega_d)^2 + (eB_z/2c)^2}$. For small variation of the gradient of the electric field $\lambda^2\nabla\nabla\varepsilon_i(\boldsymbol{r}_0) \ll \varepsilon_i(\boldsymbol{r}_0)$ (and keep in mind that the average of the linear term with a symmetric ground state wave function vanishes), we retain only the zeroth order of $\varepsilon_i(\boldsymbol{r})$, so that

$$\boldsymbol{\Omega}(t) = \frac{-e}{m^*\omega_d^2}[\varepsilon_{y'}(\boldsymbol{r}_0(t))/\lambda_-, \varepsilon_{x'}(\boldsymbol{r}_0(t))/\lambda_+, 0]. \tag{17}$$

The effective Hamiltonian holds in the lowest order of spin-orbit interaction and the lowest order of Zeeman splitting ($\Delta\boldsymbol{B}_L$ goes to zero in this limit), and it has two important features. First, the *spatially random* electric field $\boldsymbol{\varepsilon}(\boldsymbol{r})$ is now a *temporally random* magnetic field for the electron spin $\delta\boldsymbol{B}(t)$. This transformation is through the dot motion $\boldsymbol{r}_0(t)$ $[\boldsymbol{\varepsilon}(\boldsymbol{r}) \to \boldsymbol{\varepsilon}(t)]$ and the SO interaction $[\boldsymbol{\varepsilon}(t) \to \delta\boldsymbol{B}(t)]$. Second, Eqs. (15) shows that there can be *only transverse fluctuations* in the effective magnetic field since $\delta\boldsymbol{B}(t)\cdot\boldsymbol{B} = 0$ [see Fig. 1(b)]. Due to this transverse nature, there is *no pure dephasing* at the lowest order approximation.

IV. NOISE CORRELATION

To calculate the spin relaxation rate of the moving electron, we need to first obtain the temporal correlation functions $J_{ij}(t) = \langle\delta B_i\delta B_j(t)\rangle$ of the random magnetic field that leads to the spin decoherence. Recall that the random magnetic field, given by Eqs. (15) and (17), originates from the spin-orbit interaction and a random electric field, the latter from disorder in the substrate material. Thus the temporal correlation of the magnetic fluctuations comes from the spatial correlation of the random electric field. Here we choose an isotropic model for the random electrical field

$$\langle\varepsilon_i(\boldsymbol{r}_1)\varepsilon_j(\boldsymbol{r}_2)\rangle = \delta_{ij}\sigma_\varepsilon^2 f_c(\Delta r/l_\varepsilon), \tag{18}$$

where δ_{ij} is the Kronecker delta function $(i, j = x' \text{ or } y')$, σ_ε is the standard deviation of the electric field, $f_c(\Delta r/l_\varepsilon)$ is the cutoff function as listed in Table I, in which $\Delta r = |\boldsymbol{r}_1 - \boldsymbol{r}_2|$ is the distance between $\boldsymbol{r}_1$ and $\boldsymbol{r}_2$, and l_ε is the correlation length of the random field. Here, the average $\langle\cdots\rangle$ could be the average among different segments of the path when the experiment is done in a straight line, or the average in different directions when the electron is moved that way. It could also be the result of uncertainty in the driving agent, so that the time and the position of the electron do not have a one-to-one correspondence, and this variation in the electron position at a particular time gives us a degree of freedom for the averaging among different paths. Thus in the moving frame

TABLE I. Fourier transformation of different correlations.

	$f_c(r/l_\varepsilon)$	$f_c(\lvert t\rvert/\tau_c)$	$F_c(\omega)$
1	$\exp(-r/l_\varepsilon)$	$\exp(-\lvert t\rvert/\tau_c)$	$2\tau_c/\left[1+\omega^2\tau_c^2\right]$
2	$1/\left[1+r^2/l_\varepsilon^2\right]$	$1/\left[1+t^2/\tau_c^2\right]$	$\pi\tau_c\exp(-\lvert\omega\rvert\tau_c)$
3	$\exp\left(-r^2/l_\varepsilon^2\right)$	$\exp\left(-t^2/\tau_c^2\right)$	$\sqrt{\pi}\tau_c\exp\left(-\omega^2\tau_c^2/4\right)$

$$\langle\varepsilon_i(\boldsymbol{r}_0(t_1))\varepsilon_j(\boldsymbol{r}_0(t_2))\rangle = \delta_{ij}\sigma_\varepsilon^2 f_c(|t|/\tau_c), \tag{19}$$

where $t = t_2 - t_1$ and $\tau_c = l_\varepsilon/v_0$ is the correlation time. The spatially random electric field in the laboratory frame is now a temporally random electric field in the moving frame, which through Eqs. (15) and (17) becomes a temporally random magnetic field.

It is important to emphasize here that we assume the QD trajectories cannot be reproduced identically over different runs, since in realistic situations one cannot drag the electron exactly along the same path. Most importantly, the moving electron is an open system, constantly exchanging energy with the external driving agent that allows the linear motion of the QD. Since the external driver is assumed to be classical and Markovian, the electron dynamics is dissipative instead of unitary. Therefore, the resulting spin flip is not a predictable unitary spin rotation, and information is lost due to the exchange with the external reservoir.

The cross product in Eq. (15) and the arbitrary direction for the applied magnetic field mean that the magnetic correlation is in general quite complex in the $(x'y'z)$ coordinate system we have used so far. To simplify the relaxation rate calculations, we first transform to a new XYZ coordinate system, in which we require that (a) Z is along the direction of the total magnetic field $\boldsymbol{B}$ and (b) $J_{ij}(t)$ is diagonal in this coordinate system. The first requirement dictates that $\delta\boldsymbol{B}$ is always in the XY plane since $\delta\boldsymbol{B}\perp\boldsymbol{B}$. This means that $\delta B_Z = 0$ and $J_{ZZ} = 0$. The second requirement further dictates that the correlation functions are diagonal, so that there are only two independent correlation functions J_{XX} and J_{YY}.

The XYZ coordinate system can be obtained from the $(x'y'z)$ coordinates by a rotation with Euler angles φ, θ, and χ. Specifically, first rotate $(x'y'z)$ along the z axis by angle φ to $(x''y''z)$, so that the y'' axis is perpendicular to the direction of magnetic field $\hat{\boldsymbol{n}}$. Then rotate along y'' by angle θ to $(x'''y'''Z)$, so that the Z axis is in the direction $\hat{\boldsymbol{n}}$. Lastly, rotate along the Z axis by χ. Here angles φ and θ give the direction of the total magnetic field $\boldsymbol{B}$ in the $(x'y'z)$ frame, and χ is determined from the requirement $\langle\delta B_X(0)\delta B_Y(t)\rangle = 0$.

After the Euler rotations $\boldsymbol{R}_Z(\chi)\boldsymbol{R}_{y''}(\theta)\boldsymbol{R}_z(\varphi)$, the field in the XYZ coordinates is given by $\delta\boldsymbol{B}(t) = \frac{-2eB}{m^*\omega_d^2}\boldsymbol{\zeta}(t)$,

$$\zeta_X = \cos\chi(A_x + A_y) + \sin\chi(B_x + B_y),$$
$$\zeta_Y = -\sin\chi(A_x + A_y) + \cos\chi(B_x + B_y),$$

where $A_x = -\varepsilon_{x'}\cos\phi/\lambda_+$, $A_y = \varepsilon_{y'}\sin\phi/\lambda_-$, $B_x = \varepsilon_{x'}\cos\theta\sin\phi/\lambda_+$, $B_y = \varepsilon_{y'}\cos\theta\cos\phi/\lambda_-$. The condition $\langle\delta B_X \delta B_Y(t)\rangle = 0$ simply means that $\langle\zeta_X\zeta_Y(t)\rangle = 0$. Substituting each component of $\boldsymbol{\zeta}$ into the equation and considering that $\langle\varepsilon_i\varepsilon_j(t)\rangle = \delta_{ij}\sigma_\varepsilon^2 f_c(|t|/\tau_c)$, the Euler angle χ can be determined as

$$\tan 2\chi = \frac{2(\lambda_+^2 - \lambda_-^2)n_{x'}n_{y'}n_z}{\lambda_+^2\left(n_{y'}^2 - n_z^2 n_{x'}^2\right) + \lambda_-^2\left(n_{x'}^2 - n_z^2 n_{y'}^2\right)}, \tag{20}$$

where $\hat{\boldsymbol{n}}$ is the direction of the magnetic field.

With the knowledge of all the Euler angles, we can now calculate $\langle\zeta_X\zeta_X(t)\rangle$ and $\langle\zeta_Y\zeta_Y(t)\rangle$,

$$\langle\zeta_X\zeta_X(t)\rangle = \frac{1}{\Lambda_+^2}\sigma_\varepsilon^2 f_c(|t|/\tau_c),$$
$$\langle\zeta_Y\zeta_Y(t)\rangle = \frac{1}{\Lambda_-^2}\sigma_\varepsilon^2 f_c(|t|/\tau_c),$$

where the effective SO length is given by

$$\frac{2}{\Lambda_\pm^2} = \frac{1-n_{x'}^2}{\lambda_-^2} + \frac{1-n_{y'}^2}{\lambda_+^2} \pm \sqrt{\left(\frac{1-n_{x'}^2}{\lambda_-^2} + \frac{1-n_{y'}^2}{\lambda_+^2}\right)^2 - \frac{4n_{z'}^2}{\lambda_+^2\lambda_-^2}}.$$

The magnetic correlators are thus

$$J_{XX}(t) = \left[\frac{2eB\sigma_\varepsilon}{\Lambda_+ m^* \omega_d^2}\right]^2 f_c(|t|/\tau_c), \tag{21}$$

$$J_{YY}(t) = \left[\frac{2eB\sigma_\varepsilon}{\Lambda_- m^* \omega_d^2}\right]^2 f_c(|t|/\tau_c), \tag{22}$$

and $J_{ZZ}(t) = 0$, as mentioned earlier. In the following discussion, we choose the cutoff function $f_c(|t|/\tau_c)$ to be exponential for simplicity (see Appendix A for other types of cutoff functions).

V. SPIN RELAXATION

Now we study decoherence of the electron spin qubit due to Hamiltonian (14). The noise correlation time τ_c is generally much shorter than the qubit decay time (the inset of Fig. 2 shows values of τ_c). In this regime, the dynamics of the spin qubit are governed by the Bloch equations.[29] With purely transverse fluctuations, the longitudinal and transverse relaxation rates, $1/T_1$ and $1/T_2$, are[20,25,29]

$$\frac{1}{T_1} = \frac{2}{T_2} = J_{XX}^+(\omega_Z) + J_{YY}^+(\omega_Z),$$
$$J_{ij}^+(\omega) = \frac{g^2\mu_B^2}{2\hbar^2}\int_{-\infty}^{+\infty}\langle\delta B_i(0)\delta B_j(t)\rangle\cos(\omega t)dt. \tag{23}$$

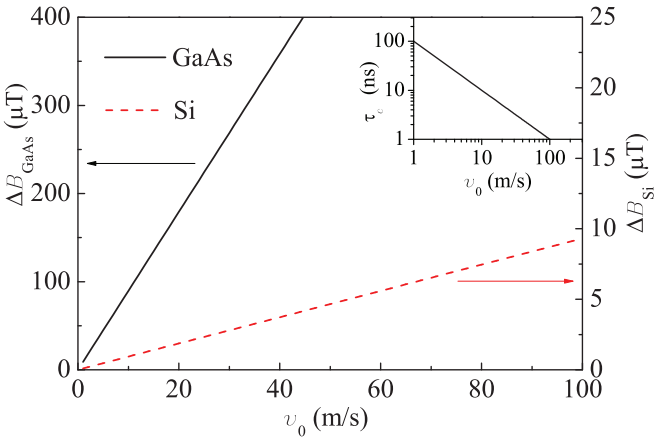

FIG. 2. (Color online) ΔB as a function of moving velocity for GaAs (solid line) QD with $\beta = 300$ m/s and Si (dashed line) QD with $\alpha = 5$ m/s. The inset gives the bath correlation time τ_c.

Using Eq. (A2) and its J_{YY} correspondent, we obtain

$$\frac{1}{T_1} = \left[\frac{2e\sigma_\varepsilon}{\hbar\omega_d^2}\right]^2 \frac{\omega_Z^2\tau_c}{1+\omega_Z^2\tau_c^2} F_{SO}(\theta,\phi), \tag{24}$$

$$F_{SO} = [(\beta^2+\alpha^2)(1+\cos^2\theta) + 2\alpha\beta\sin^2\theta\cos 2\phi]. \tag{25}$$

Here θ and ϕ are the polar and azimuthal angles of $\boldsymbol{B}$ in the $x'y'z'$ coordinates.

Before delving into the numerics we first discuss some qualitative features of the spin relaxation rate here. Firstly, $1/T_1 \propto 1/\omega_d^4$. This strong dependence on the QD confinement means that this spin relaxation channel can be suppressed by having strong confinement for the QD. Secondly, $1/T_1 \propto \sigma_\varepsilon^2$. The origin of the static disorder would determine the magnitude here. For example, in a modulation doped GaAs structure, $\delta V \sim 20$ mV[30] and $l_\varepsilon \sim 0.1\mu$m,[30] so that $\sigma_\varepsilon = \delta V/l_\varepsilon \sim 200$ kV/m. On the other hand, for an undoped top-gate structure in Si,[31] there could be disorder from defects in the barrier, though its characteristic length and strength are unknown (most probably much smaller than in the modulation doped structures). Our numerical estimates below use parameters from the modulation doped structures.

The SO coupling dependence of $1/T_1$ is contained in F_{SO} in terms of α and β, the Rashba and Dresselhaus SO coupling strength. These parameters are materials- and device-specific. In Si $\beta = 0$, while in GaAs $\beta_{GaAs} = 300$ m/s is fixed (see Appendix B). In both materials α is dependent on the particular quantum well structure and doping.

The dependence on the direction of magnetic field $\boldsymbol{B}$ by $1/T_1$ is also contained in F_{SO}, in terms of the polar and azimuthal angles θ and ϕ. For example, for a perpendicular field ($\boldsymbol{B} \parallel [001]$), $F_{SO} = 2(\beta^2+\alpha^2)$. For an in-plane field, $F_{SO} = \beta^2 + \alpha^2 + 2\alpha\beta\cos 2\phi$. Thus, the decay rate in a perpendicular field is always larger than if the field is in-plane $(1/T_1)_{\text{perp}} \geqslant (1/T_1)_{\text{in-plane}}$.

In the case of an in-plane magnetic field, the spin relaxation rate $1/T_1$ has a sinusoidal dependence on the azimuthal angle ϕ of the $\boldsymbol{B}$ field. The minimum rate is $1/T_1 = [2e\sigma_\varepsilon(\beta-\alpha)/(\hbar\omega_d^2)]^2\omega_Z^2\tau_c/(1+\omega_Z^2\tau_c^2)$ (assuming $\alpha\beta > 0$), when the $\boldsymbol{B}$ field is along the y axis ($\phi = \pi/2$). Thus, in the special case

when $\alpha = \beta$ and $\phi = \pi/2$ (or $\alpha = -\beta$ and $\phi = 0$), $1/T_1 = 0$. In other words, since $\Delta \boldsymbol{B}$ is along the y (x) axis when $\alpha = \beta$ ($\alpha = -\beta$) [c.f. Eq. (10)], spin relaxation due to QD motion *vanishes* if the applied magnetic field $\boldsymbol{B}_0$ is along y for $\alpha = \beta$ (or along the x axis for $\alpha = -\beta$). Such special cases ($\alpha = \pm\beta$) have been discussed previously in the context of spin relaxation due to phonon emission.[20,32] Note that Hamiltonian H in Eq. (1) conserves the spin component $\sigma_{y(x)}$ for $\alpha = \beta$ ($\alpha = -\beta$) and $\boldsymbol{B}_0 \parallel y\,(x)$. This spin conservation results in T_1 being infinite to all orders in the SO interaction Hamiltonian (9). Meanwhile, decoherence rate $1/T_2$ reduces to the next order contribution of Eq. (4), in the form of pure dephasing.

The dependence on the magnitude of $\boldsymbol{B}$ and velocity $\boldsymbol{v}_0$ by $1/T_1$ is contained in $\omega_Z^2\tau_c/(1+\omega_Z^2\tau_c^2)$ of Eq. (24). Here we first estimate the magnitude of ΔB [c.f. Eq. (10)]. In Fig. 2, we plot ΔB as a function of velocity $|\boldsymbol{v}_0|$ for GaAs and Si QDs. ΔB is two orders of magnitude larger in GaAs than in Si, but still negligible if a strong magnetic field (order of Tesla) is applied. We discuss the high and low field cases separately as follows.

A. High field and slow moving limit

For a strong applied magnetic field ($B \geqslant 1$ T) and a slow moving QD (1 nm/ns $< v_0 <$ 100 nm/ns), $\Delta \boldsymbol{B}$ can be neglected, and the condition $\omega_Z\tau_c \gg 1$ is satisfied. In this limit, the ω_Z (or B) dependence cancels out in Eq. (24). $1/T_1$ depends linearly on the speed v_0 of the QD, and is independent of the direction of the motion (since ΔB is neglected).

We carry out numerical calculations on two representative QD structures, one in GaAs/$Al_{1-x}Ga_xAs$, the other in Si/SiGe. In both cases, the dot confinement energies are set at $\hbar\omega_d =$ 1 meV and 3 meV, and the applied magnetic field is $B_0 = 1$ T. For the GaAs QD, we use the bulk g factor $g = -0.44$, and the electron effective mass $m^* = 0.067m_0$, where m_0 is the free electron rest mass. For the Si QD, $g = 2$, $m^* = 0.19\ m_0$, and the Rashba SO coupling strength is chosen to be $\alpha_{Si} =$ 5 m/s.[33–35] Figure 3 shows the spin relaxation rate $1/T_1$ as a

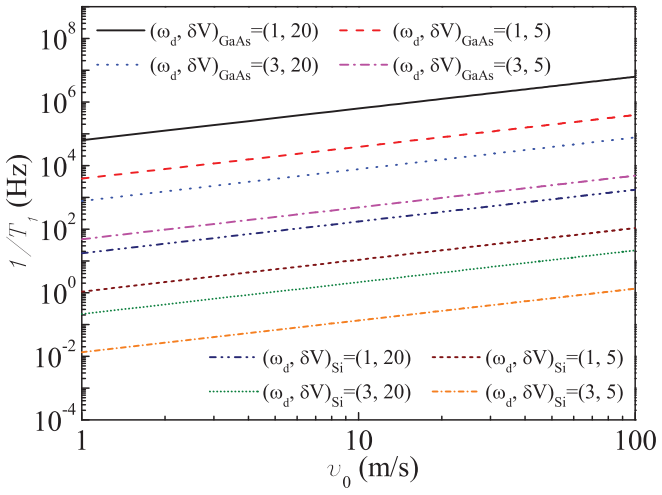

FIG. 3. (Color online) Spin relaxation rate $1/T_1$ as a function of the QD velocity for GaAs QDs with $\beta = 300$ m/s and Si QDs with $\alpha = 5$ m/s (with an in-plane magnetic field). Here ω_d and δV are in units of meV and mV.

function of the QD speed in an in-plane $\boldsymbol{B}$ field, when

$$\left.\frac{1}{T_1}\right|_{\text{in-plane}} = \frac{v_0}{l_\varepsilon}\left[\frac{2e\sigma_\varepsilon}{\hbar\omega_d^2}\right]^2(\beta^2+\alpha^2+2\alpha\beta\cos 2\phi). \tag{26}$$

For a moving GaAs QD, we find that T_1 ranges from μs to 10 ms. For a Si QD, $T_1 > 1$ ms because of the weaker SO coupling. In terms of the moving distance $(v_0T_1)_{\text{in-plane}}$, spin coherence is lost in as short as μm in GaAs and mm in Si for a dot speed of 10 nm/ns. Clearly, while the spin relaxation times here are still much longer than those in a 2DEG, the QD motion does present a serious threat to the coherence of the spin qubit, especially in modulation doped GaAs heterostructures.

B. Low field and fast moving limit

If the magnetic field is low, and/or the QD motion is fast (but still adiabatic), so that $\omega_Z\tau_c \ll 1$, the spin relaxation rate is

$$\frac{1}{T_1} = \left[\frac{2e\sigma_\varepsilon}{\hbar\omega_d^2}\right]^2 F_{SO}(\theta,\phi)\omega_Z^2\tau_c. \tag{27}$$

If the applied field B_0 is much larger than ΔB, so that $g\mu_B\Delta B/\hbar \ll \omega_Z \ll \tau_c^{-1}$, we obtain $1/T_1 \propto 1/v_0$, indicating motional narrowing. Whereas, if $B_0 = 0$, only $\Delta \boldsymbol{B}$ contributes to the spin splitting, with $\theta = \pi/2$ and $\beta_- \tan\phi = \beta_+ \cot\phi_v$. Now $\omega_Z^2\tau_c = (2m^*/\hbar)^2 v_0 l_\varepsilon F_v(\phi_v)$, where $F_v(\phi_v) = (\beta^2+\alpha^2+2\alpha\beta\cos 2\phi_v)$. Interestingly, this ϕ_v dependence is completely canceled by that in F_{SO}, so that

$$\frac{1}{T_1} = v_0 l_\varepsilon[4e\sigma_\varepsilon m^*(\beta^2-\alpha^2)/(\hbar\omega_d)^2]^2. \tag{28}$$

In other words, when no magnetic field is applied, $1/T_1$ depends linearly on the speed v_0 of the QD motion and is independent of the direction ϕ_v of the motion.

As an example we consider an SAW-confined electron in GaAs. Here the QD moves fast, at the speed of sound $v_0 = v_{\text{SAW}} = 3000$ m/s, so that the low-field limit $\omega_Z\tau_c \ll 1$ is satisfied even for $B_0 \simeq 1$ T. The electron should still remain in the ground orbital state, however, while the motion-induced magnetic field is now $\Delta \boldsymbol{B} \sim 0.02$ T. The spin relaxation rate should have a weak dependence on the direction of the motion when B_0 and ΔB are comparable. The confinement potential for an electron in an SAW is dependent on the driving intensity P_{SAW}, with $\omega_d \sim 1$ meV (see Appendix B). Using parameters for modulation doped samples, $l_\varepsilon \sim 0.1\mu$m and $\sigma_\varepsilon \sim 200$ kV/m, we estimate that $1/T_1 \sim 10^8$ Hz in a strong in-plane magnetic field ($B_0 \gg \Delta B$, $\beta = 300$ m/s and $\alpha = 0$) and $1/T_1 \sim 10^5$ Hz when $B_0 = 0$. These rates can be reduced by having a larger ω_d (with higher SAW driving intensity and/or higher frequency), and most importantly, using a less disordered sample with smaller σ_ε.

VI. DISCUSSION AND CONCLUSION

It is important to emphasize here that the static disorder potential is not the reservoir by itself. It is the external driver that energizes the reservoir. The disorder is what allows the spin to exchange energy with the reservoir: It modifies the mode functions of the electromagnetic environment. As we mentioned at the beginning of the paper, we assume that the

driving agent is classical and Markovian, so that whatever information goes into the driving agent is lost. In other words, we have performed a phenomenological study of an open system where energy is not conserved. This calculation does not treat the external driving agent in a quantum mechanical fashion: It only energizes the disorder through motion, but does not have any internal structure. A definitive and complete study of the spin-reservoir exchange requires quantization of the nonequilibrium external driving agent, which is beyond the scope of the current study. However, we hope this work could act as a catalyst for further theoretical and experimental studies on this interesting problem.

As we mentioned before, for confined electron spins HF-induced dephasing is the most important decoherence mechanism. For a moving but confined electron spin, however, this dephasing is suppressed due to motional narrowing: $1/T_2^* \propto 1/v$ (see Appendix C). For example, in a QD with a 1 meV confinement energy in GaAs, the HF-induced dephasing time goes up from 30 ns in a stationary QD to $> 1\ \mu$s when the dot speed is 20 m/s, while at this speed the spin relaxation due to SO coupling is already faster: $T_1 \sim 1\ \mu$s. Thus even with only a moderate speed of motion, the HF-induced dephasing is already superseded by the SO-induced relaxation as the main source of decoherence for the electron spin.

The model calculation presented in this manuscript focuses on the effect of the momentum scattering of the electron due to the random electrical potential in the plane of the quantum dot motion. In our calculation we did not include the possible effect of a random component of the Rashba spin-orbit coupling due to the random electric field along the growth direction.[23,24] This choice is a reflection of our assumption that the growth direction confinement is much stronger than the in-plane confinement, so that the relative fluctuation of the spin-orbit coupling should be weak compared to the existing coupling itself. If this assumption does not hold, the random field along the growth direction would have to be properly taken into account as well.

In conclusion, we have studied electron spin relaxation in a moving QD. The relaxation mechanism we studied originates from momentum scattering and SO interaction. At the lowest order, it is a longitudinal relaxation channel, so that $T_2 = 2T_1$. The relaxation rate is inversely proportional to the fourth power of the confinement energy, so that spin decoherence is faster for larger quantum dots. For high-field slow motion or very-low-field fast motion, the decoherence rate increases linearly with the QD speed. Quantitatively, in modulation-doped GaAs heterostructures this can be an important spin decoherence channel, where spin relaxation time can be as short as sub-μs and as long as ms, depending on the QD confinement strength and the magnitude of the random potential. For modulation doped Si/SiGe QDs the spin relaxation rate is generally several orders of magnitude slower. However, compared to known spin decoherence channels in Si, this relaxation can still be quite significant.

ACKNOWLEDGMENTS

We thank support by US ARO (W911NF0910393), DARPA QuEST through AFOSR, and NSF PIF (PHY-1104672), and useful discussions with Seigo Tarucha and Eugene Sherman.

TABLE II. Approximations of $F_c(\omega)$ in different limits.

$F_c(\omega)$	$\omega\tau_c \gg 1$	$\omega\tau_c \ll 1$
1	$2/(\omega^2\tau_c)$	$2\tau_c$
2	$\pi\tau_c \exp(-\lvert\omega\rvert\tau_c)$	$\pi\tau_c$
3	$\sqrt{\pi}\tau_c \exp\left(-\omega^2\tau_c^2/4\right)$	$\sqrt{\pi}\tau_c$

APPENDIX A: EFFECTS OF THE DIFFERENT CUTOFF FUNCTIONS

The decoherence of the moving electron spin $\boldsymbol{S} = \boldsymbol{\sigma}/2$ is governed by the Hamiltonian (14). In general, the noise correlation time τ_c is much shorter than the spin decay time. In this regime, the dynamics and relaxation of the spin is governed by the Bloch equation.[29] With purely transverse fluctuations, the longitudinal and transverse relaxation rates, $1/T_1$ and $1/T_2$, are[25,29]

$$\frac{1}{T_1} = \frac{2}{T_2} = J_{XX}^{+}(\omega_Z) + J_{YY}^{+}(\omega_Z), \tag{A1}$$

where the magnetic correlation function in the frequency domain is $J_{ij}^{+}(\omega) = \frac{g^2\mu_B^2}{2\hbar^2}\int_{-\infty}^{+\infty}\langle\delta B_i(0)\delta B_j(t)\rangle\cos(\omega t)dt$. Thus

$$J_{XX}^{+}(\omega) = \frac{2(\omega_Z e\sigma_\varepsilon)^2}{\left(\Lambda_+ m^*\omega_d^2\right)^2}\int_{-\infty}^{+\infty} f_c(\lvert t\rvert/\tau_c)\cos(\omega t)dt, \tag{A2}$$

and $J_{YY}^{+}(\omega)$ is obtained from Eq. (A2) by substituting $\Lambda_+ \to \Lambda_-$. The relaxation rate is then

$$\frac{1}{T_1} = 2\left[\frac{\omega_Z e\sigma_\varepsilon}{\hbar\omega_d^2}\right]^2 F_{SO}(\theta,\phi)F_c(\omega_Z), \tag{A3}$$

where $F_c(\omega)$ is the Fourier transform of $f_c(\lvert t\rvert/\tau_c)$, as shown in Table I.

As shown in Table II, different types of cutoff functions are very similar at the low-field-fast-motion limit, but behave dramatically differently in the high-field-slow-motion regime. We thus focus on the latter regime, and plot the relaxation rate as a function of the QD velocity for different types of correlations in Fig. 4. Overall, $1/T_1$ is a monotonically increasing function of the speed of the QD motion, no matter which type of correlation function is used (in particular, $1/T_1$ is a linear function of v_0 for the type-1 correlation function). However, quantitatively the relaxation is completely suppressed for the type-2 and -3 cutoff functions because of the exponential suppression from $\exp(-\lvert\omega_Z\rvert\tau_c)$ and $\exp(-\omega_Z^2\tau_c^2/4)$ (with a 1 T external field in GaAs and a τ_c between 1 and 100 ns, we are in the limit of $\omega_Z\tau_c \gg 1$). In these cases, spin decoherence is probably dominated by higher-order dephasing processes due to the SO coupling.[36]

APPENDIX B: MEASURING SPIN-ORBIT COUPLING STRENGTH USING CARRIERS TRAPPED BY A SAW

A surface acoustic wave (SAW) in GaAs induces a piezoelectric field in the form of $E_{\mathrm{SAW}}\cos(k_{\mathrm{SAW}}x - \omega_{\mathrm{SAW}}t)$, where $k_{\mathrm{SAW}} = 2\pi/\lambda_{\mathrm{SAW}}$ is the wave vector, and ω_{SAW} is the SAW frequency. The troughs of this propagating electric potential can act as a moving QD for electrons, with a velocity at the speed of sound. In the moving frame the confinement potential is approximated as $E_{\mathrm{SAW}}\cos(k_{\mathrm{SAW}}x) \approx E_{\mathrm{SAW}}(1 - k_{\mathrm{SAW}}^2x^2/2)$

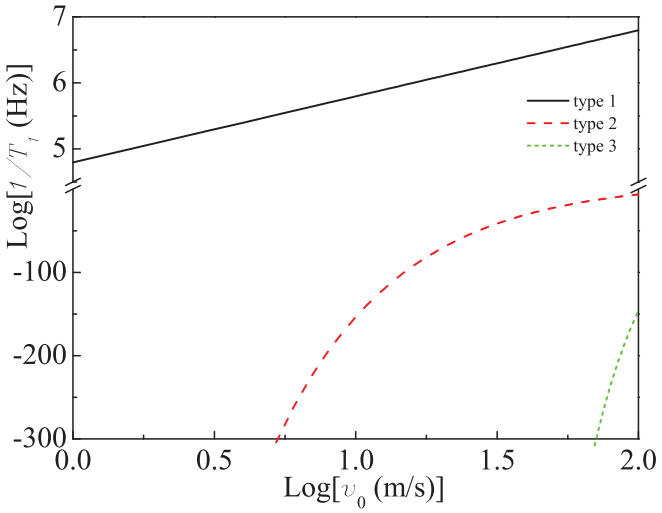

FIG. 4. (Color online) Spin relaxation rate $1/T_1$ as a function of the velocity in GaAs QDs for different types of correlation functions (in-plane field $B = 1$ T, $\alpha = 0$, and $\beta = 300$ m/s).

assuming $k_{\mathrm{SAW}}x \ll 1$. Therefore, the confinement energy can be estimated as $\omega_d = 2\pi\sqrt{E_{\mathrm{SAW}}/m_e^*}/\lambda_{\mathrm{SAW}} \propto \sqrt{P_{\mathrm{SAW}}}/\lambda_{\mathrm{SAW}}$, where $m_e^* = 0.067m_e$ is the electron effective mass, and P_{SAW} is the RF power that generates the SAW. According to Ref. 14, $E_{\mathrm{SAW}}[eV] = 2/25 \times 10^{(P[dBm]-23)/20}$. We can thus estimate E_{SAW} and ω_d, as shown in Table III.

SAW-trapped electrons can help determine the spin-orbit coupling strength in the underlying material. For example, in GaAs the electrons and holes that are photoexcited can be picked up by a SAW. The spatial distribution of electron spins can then be measured by photoluminescence (specifically polarization of the emitted photons) or magneto-optic Kerr rotation.[13,16] In terms of Kerr rotation, for instance, the spin distribution is expressed as $\theta_K(d) = \theta_0 e^{-d/v_0T_2}\cos(\omega_Z d/v_0) = \theta_0 e^{-d/L_s}\cos(2\pi\kappa d)$, where d is the distance from the origin where the excitons are generated, $L_s = v_0T_2$ is the spin decay length, and $\kappa = \omega_Z/(2\pi v_0)$ is the spatial precession frequency. In the absence of an applied magnetic field, the spin precession frequency $\omega_Z = g\mu_B\Delta B/\hbar$ is completely determined by the motion-induced magnetic field $\Delta\boldsymbol{B}$,

$$\Delta\boldsymbol{B} = \frac{2m^*}{g\mu_B}(\beta_- v_{0y}, \beta_+ v_{0x}, 0). \tag{B1}$$

This field has been measured to be sizable (25 mT in Ref. 13 for GaAs), because of the high speed of the QD motion. Based on Eq. (B1) and $\kappa = \omega_Z/(2\pi v_0) = g\mu_B\Delta B/(hv_0)$, one can determine the SO coupling constants by measuring the spatial precession frequency κ experimentally.[16] This leads to an upper limit of the Dresselhaus SO coupling constant at $\beta = 300$ m/s, which is consistent with other recent experiments.[16,37,38] However, this β value is smaller than what was used in earlier theoretical calculations.[1,28,39] More experimental studies would be needed to clarify this issue.

TABLE III. Estimation of the confinement energies for different driving power.

P (dBm)	E_{SAW} (meV)	ω_d (meV)
3	8	0.5
13	25.3	0.9
23	80	1.6

APPENDIX C: MOTIONAL NARROWING OF NUCLEAR SPIN INDUCED DEPHASING

As we have discussed in the main text, the main decoherence channel for a confined electron spin in a finite field is the hyperfine interaction induced pure dephasing,[18,19] while spin relaxation of free electrons and holes in semiconductors is dominated by spin-orbit interaction.[22,23] Here we show how the effect of hyperfine interaction is strongly suppressed by motional narrowing for a moving electron spin qubit with controlled motion.

The contact hyperfine interaction for the electron in a quantum dot can be written as

$$H_{HF} = \sum A_i \boldsymbol{S}\cdot\boldsymbol{I}_i, \tag{C1}$$

where $A_i = A|\psi(\boldsymbol{r}_i)|^2$ is the hyperfine coupling constant at lattice site i [with A being the total hyperfine coupling strength and $\psi(\boldsymbol{r})$ the electron envelope function in the quantum dot]. In GaAs, for example, $A = 92$ μeV, $\boldsymbol{S}$ is the electron spin, and $\boldsymbol{I}_i$ is the nuclear spin at lattice site i. Since nuclear spin evolves much more slowly compared to the electron spin, we can treat it semiclassically as an Overhauser field:

$$\boldsymbol{B}_N = \sum A_i \boldsymbol{I}_i. \tag{C2}$$

In the presence of an external magnetic field along the z direction, we can focus on the z component of the Overhauser field B_{Nz} (let $g\mu_B = 1$):

$$H = (B_0 + B_{Nz})S_z. \tag{C3}$$

Since nuclear spins are randomly oriented in a sample at any reasonable experimental temperature, the electron spin would experience a fluctuating magnetic field as it moves, and undergo dephasing accordingly in the off-diagonal element of the electron spin density matrix: $\rho_{\uparrow\downarrow}(t) = \rho_{\uparrow\downarrow}(0)e^{-\delta\phi(t)}$. Here the phase diffusion is given by

$$\delta\phi(t) = \frac{1}{2\hbar^2}\int_0^\infty d\omega\, S_{B_N}(\omega)\left(\frac{\sin\omega t/2}{\omega/2}\right)^2. \tag{C4}$$

Here the nuclear field spectral density $S_{B_N}(\omega)$ is

$$S_{B_N}(\omega) = \frac{1}{2\pi}\int_{-\infty}^{\infty} dt e^{i\omega t}\langle B_{Nz}(t)B_{Nz}(0)\rangle.$$

For a moving quantum dot in GaAs with a trajectory $\boldsymbol{r}(t) = \boldsymbol{r}(0) + \boldsymbol{v}t$, and assuming that any two different nuclear spins are completely uncorrelated, we find

$$\langle B_{Nz}(t)B_{Nz}\rangle = \frac{5}{4}A^2\Omega\int d\boldsymbol{R}\,|\psi(\boldsymbol{R}-\boldsymbol{r}(t))|^2|\psi(\boldsymbol{R}-\boldsymbol{r}(0))|^2,$$

where we have used $\langle I_z^2\rangle = 5/4$ for GaAs, and Ω is the volume of a lattice unit cell. For simplicity, we calculate the integral using a Gaussian envelope wave function for the electron with

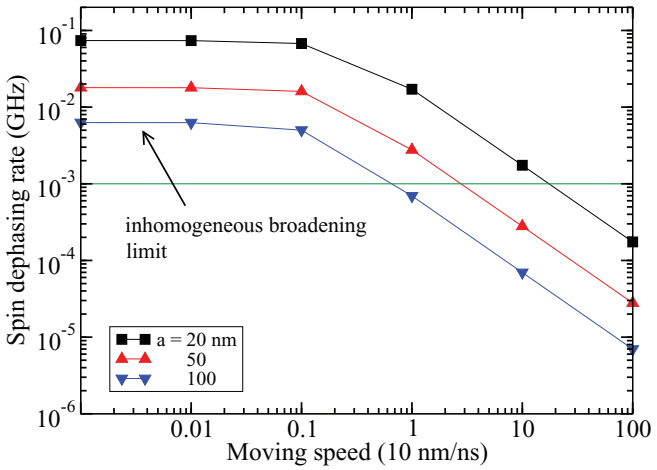

FIG. 5. (Color online) Spin dephasing time T_2^* as a function of the speed v of a moving GaAs QD. The horizontal line indicates a dephasing time of 1 μs.

radius a, and obtain the spectral density as

$$S_{B_N}(\omega) = \frac{5A^2}{16\pi^2}\frac{\Omega}{a^3}\frac{a}{v}e^{-(\frac{\omega a}{v})^2/2}, \tag{C5}$$

where a is the radius of the quantum dot, and v is the speed of QD motion. Now the electron spin phase diffusion can be calculated:

$$\delta\phi(t) = \frac{5A^2}{16\pi^2\hbar^2}\frac{\Omega}{a^3}\frac{at}{v}\int_0^\infty d\theta e^{-2(a/vt)^2\theta^2}\left(\frac{\sin\theta}{\theta}\right)^2. \tag{C6}$$

The integral here can be evaluated numerically given dot radius a and dot speed v. In Fig. 5 we plot the spin dephasing time T_2^* as a function of the speed v of a moving GaAs QD. Here T_2^* is defined according to the equality $\delta\phi(T_2^*) = 1$. When the motion speed goes to zero, we obtain the inhomogeneous broadening for a fixed QD, with dephasing time between 10 and 100 ns. When the speed v is large (>10 m/s), the dephasing becomes suppressed. The electron samples a larger number of nuclear spins as it moves faster, and the effect of the random nuclear field averages out, which is a typical manifestation of the motional narrowing effect. A close inspection of the high-speed results in Fig. 5 and Eq. (C6) shows that for large v, the dephasing time T_2^* due to hyperfine interaction is proportional to v, so the dephasing rate is proportional to $1/v$, while Eq. (24) shows that the spin relaxation rate due to spin-orbit interaction is proportional to v. Comparing numerical results given in Figs. 3 and 5, we can see that in GaAs, when the dot speed exceeds 10 m/s to 100 m/s, the nuclear spin induced dephasing becomes less important than the spin-orbit and random potential induced relaxation.

In the discussion here about nuclear spin induced dephasing, we have considered only the lowest order effect of the nuclear spins, i.e., the inhomogeneous broadening induced by random but static nuclear polarization. We have not considered pure dephasing due to nuclear spin dynamics. How the nuclear spin dynamics is affected by the dot motion, and how the dynamics would feed back into the electron spin coherence/decoherence, remain open theoretical questions. Qualitatively, nuclear spin dynamics induced electron spin decoherence is generally slower than dephasing due to inhomogeneous broadening. Thus the crossover we study here should be a reliable indication of the overall competition between hyperfine interaction and spin-orbit interaction.

*peihaohu@buffalo.edu

[1] R. Hanson, L. P. Kouwenhoven, J. R. Petta, S. Tarucha, and L. M. K. Vandersypen, Rev. Mod. Phys. **79**, 1217 (2007).
[2] J. J. L. Morton, D. R. McCamey, M. A. Eriksson, and S. A. Lyon, Nature (London) **479**, 345 (2011).
[3] D. Loss and D. P. DiVincenzo, Phys. Rev. A **57**, 120 (1998).
[4] A. Imamoglu, D. D. Awschalom, G. Burkard, D. P. DiVincenzo, D. Loss, M. Sherwin, and A. Small, Phys. Rev. Lett. **83**, 4204 (1999).
[5] X. Hu, Y.-x. Liu, and F. Nori, Phys. Rev. B **86**, 035314 (2012).
[6] M. Friesen, A. Biswas, X. Hu, and D. Lidar, Phys. Rev. Lett. **98**, 230503 (2007).
[7] C. H. W. Barnes, J. M. Shilton, and A. M. Robinson, Phys. Rev. B **62**, 8410 (2000).
[8] A. J. Skinner, M. E. Davenport, and B. E. Kane, Phys. Rev. Lett. **90**, 087901 (2003).
[9] A. D. Greentree, J. H. Cole, A. R. Hamilton, and L. C. L. Hollenberg, Phys. Rev. B **70**, 235317 (2004).
[10] J. M. Taylor, H. A. Engel, W. Dur, A. Yacoby, C. M. Marcus, P. Zoller, and M. D. Lukin, Nat. Phys. **1**, 177 (2005).
[11] K. D. Petersson, L. W. McFaul, M. D. Schroer, M. Jung, J. M. Taylor, A. A. Houck, and J. R. Petta, Nature (London) **490**, 380 (2012).
[12] S. Oh, L.-A. Wu, Y.-P. Shim, J. Fei, M. Friesen, and X. Hu, Phys. Rev. A **84**, 022330 (2011).
[13] J. A. H. Stotz, R. Hey, P. V. Santos, and K. H. Ploog, Nat. Mater. **4**, 585 (2005).
[14] S. Hermelin, S. Takada, M. Yamamoto, S. Tarucha, A. D. Wieck, L. Saminadayar, C. Bauerle, and T. Meunier, Nature (London) **477**, 435 (2011).
[15] R. P. G. McNeil, M. Kataoka, C. J. B. Ford, C. H. W. Barnes, D. Anderson, G. A. C. Jones, I. Farrer, and D. A. Ritchie, Nature (London) **477**, 439 (2011).
[16] H. Sanada, T. Sogawa, H. Gotoh, K. Onomitsu, M. Kohda, J. Nitta, and P. V. Santos, Phys. Rev. Lett. **106**, 216602 (2011).
[17] M. Yamamoto, S. Takada, C. Bauerle, K. Watanabe, A. D. Wieck, and S. Tarucha, Nat. Nanotech. **7**, 247 (2012).
[18] L. Cywinski, W. M. Witzel, and S. Das Sarma, Phys. Rev. Lett. **102**, 057601 (2009).
[19] H. Bluhm, S. Foletti, I. Neder, M. Rudner, D. Mahalu, V. Umansky, and A. Yacoby, Nat. Phys. **7**, 109 (2011).
[20] V. N. Golovach, A. Khaetskii, and D. Loss, Phys. Rev. Lett. **93**, 016601 (2004).
[21] F. Meier and B. P. Zakharchenia, *Optical Orientation* (North-Holland, Amsterdam, 1984).
[22] I. Zutic, J. Fabian, and S. Das Sarma, Rev. Mod. Phys. **76**, 323 (2004).
[23] V. K. Dugaev, E. Y. Sherman, V. I. Ivanov, and J. Barnas, Phys. Rev. B **80**, 081301 (2009).

[24]M. M. Glazov, E. Y. Sherman, and V. K. Dugaev, Physica E **42**, 2157 (2010).
[25]M. Borhani, V. N. Golovach, and D. Loss, Phys. Rev. B **73**, 155311 (2006).
[26]V. N. Golovach, M. Borhani, and D. Loss, Phys. Rev. B **74**, 165319 (2006).
[27]I. L. Aleiner and V. I. Fal'ko, Phys. Rev. Lett. **87**, 256801 (2001).
[28]P. Stano and J. Fabian, Phys. Rev. Lett. **96**, 186602 (2006).
[29]C. P. Slichter, *Principles of Magnetic Resonance* (Springer-Verlag, Berlin, 1980).
[30]J. A. Nixon and J. H. Davies, Phys. Rev. B **41**, 7929 (1990).
[31]B. M. Maune, M. G. Borselli, B. Huang, T. D. Ladd, P. W. Deelman, K. S. Holabird, A. A. Kiselev, I. Alvarado-Rodriguez, R. S. Ross, A. E. Schmitz *et al*., Nature (London) **481**, 344 (2012).
[32]J. Schliemann, J. C. Egues, and D. Loss, Phys. Rev. Lett. **90**, 146801 (2003).
[33]Z. Wilamowski, W. Jantsch, H. Malissa, and U. Rössler, Phys. Rev. B **66**, 195315 (2002).
[34]C. Tahan and R. Joynt, Phys. Rev. B **71**, 075315 (2005).
[35]M. Prada, G. Klimeck, and R. Joynt, New J. Phys. **13**, 013009 (2011).
[36]Y. Makhlin and A. Shnirman, Phys. Rev. Lett. **92**, 178301 (2004).
[37]M. Studer, M. P. Walser, S. Baer, H. Rusterholz, S. Schon, D. Schuh, W. Wegscheider, K. Ensslin, and G. Salis, Phys. Rev. B **82**, 235320 (2010).
[38]D. M. Zumbuhl, J. B. Miller, C. M. Marcus, K. Campman, and A. C. Gossard, Phys. Rev. Lett. **89**, 276803 (2002).
[39]C. Tahan, M. Friesen, and R. Joynt, Phys. Rev. B **66**, 035314 (2002).